On the hardening of ionising photons in HII regions across spiral disks

José M. Vílchez

I.A.A. - CSIC (Granada)

VIII Estallidos Workshop, 8-10 March 2010

Star formation in HII regions: e.g. M33

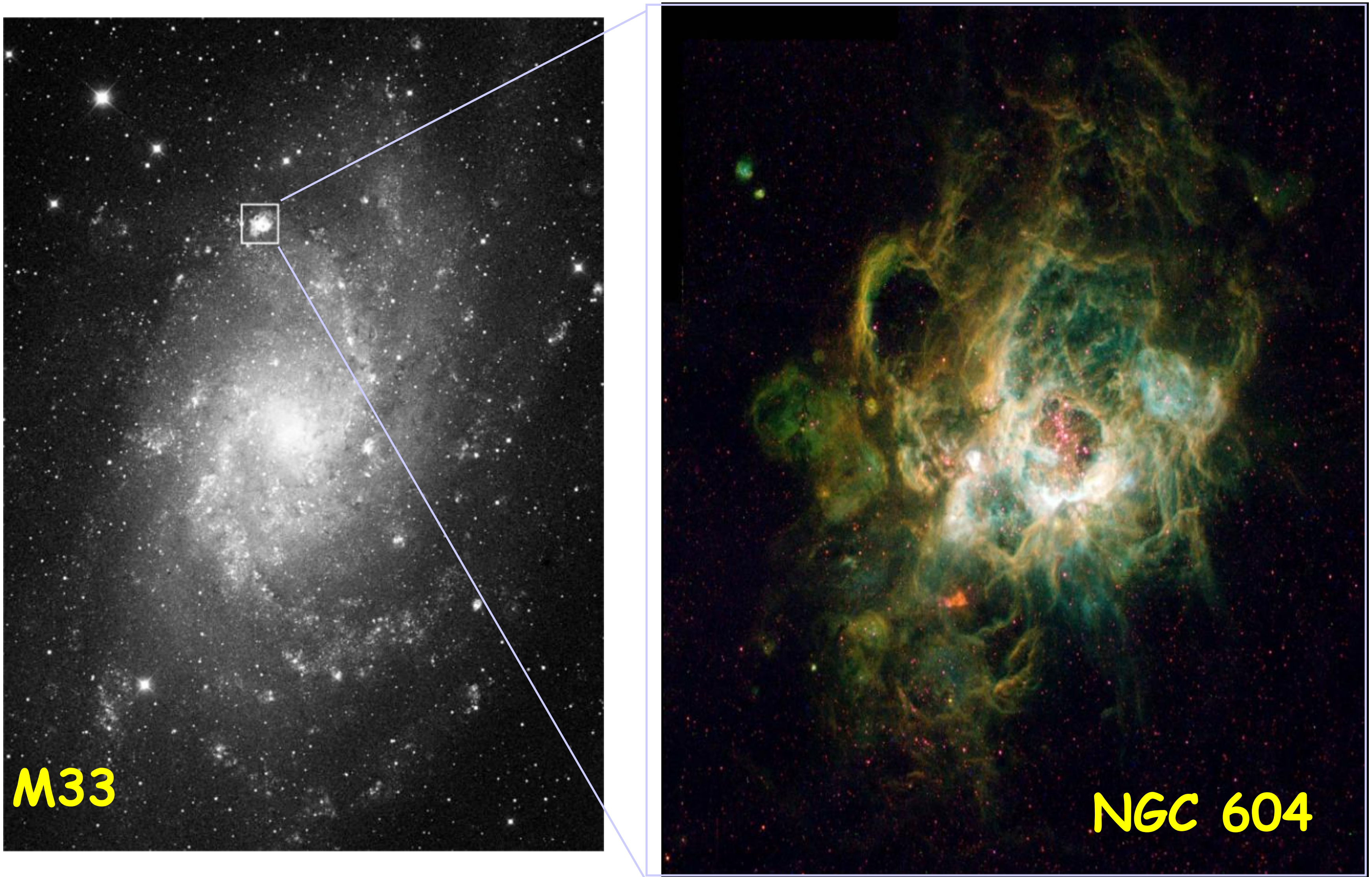

M33 in the Local Group : triangulum galaxy

Pioneering spectroscopic observations of *Extragalactic* HII Regions

THE SPECTRA OF THE EMISSION NEBULOSITIES IN MESSIER 33

LAWRENCE H. ALLER[1]

ABSTRACT

The emission nebulosities in Messier 33 are similar in spectral characteristics to those of our own Galaxy and to the low-excitation planetary IC 418. The ratio of λ 5007/λ 3727 is found to be the most reliable excitation criterion for these nebulosities. The available evidence suggests that in most of these nebulosities the oxygen is predominantly in the singly ionized condition.

Astronomers have for some time recognized the presence of bright-line nebulosities in external galaxies. Seyfert[2] discovered emission nebulosities in M 101; Babcock[3] found faint emission patches at a considerable distance from the nucleus of the Andromeda nebula; while Mayall[4] has recently given a comprehensive survey of the occurrence of λ 3727 of [*O* II], and other lines as well, in the spectra of extragalactic nebulae.

Bright lines in the nebulous condensations of Messier 33 (NGC 604, 588, and 595) have been observed by Slipher,[5] by Pease,[6] and by Hubble.[7] A preliminary list of the emission patches observed in the rotational study of this spiral has been given elsewhere.[8] However, a more detailed and complete description of these emission nebulosities with respect to their excitation characteristics seems worth while. Accordingly, rough intensity estimates of the bright lines have been made whenever practicable.

The small dispersion of the spectrograms and the graininess of the fast emulsion used rendered impracticable the ordinary methods of spectrophotometry. Intensities, estimated with the aid of scale plates, seemed the best solution of the problem. Dr. Mayall and the writer made the scale plates in the following fashion.

While the spectrograph was off the telescope, we mounted an iris diaphragm between the spark and the slit. By varying the apertures of the iris diaphragm, which had been calibrated with a photoelectric cell in the laboratory,[9] we were able to make a series of exposures upon each type of emulsion with a fixed exposure time and with known intensity ratios. We developed the scale plates in the same way as the nebular plates. We then estimated the relative intensities of the lines in the nebular spectrum simply by comparing them with the lines on the scale plate.

Line intensities measured in this way, although better than estimates made on an arbitrary scale, may be affected by large systematic errors. The individual exposures were one second on the scale plates and several hours on the nebular spectra. The density-intensity curves derived from the former may not, therefore, be quite valid for the latter. More serious is the circumstance that the continuous background is often quite strong, and the scale-plate method makes no allowance for emission lines superposed on

[1] Society of Fellows, Harvard University.

[2] *Ap. J.*, **91**, 261, 1940.

[3] *Lick Obs. Bull.*, **19**, 41, 1939 (No. 498). [4] *Lick Obs. Bull.*, **19**, 33, 1939 (No. 497).

[5] *Pop. Astr.*, **23**, 23, 1915; *Proc. Amer. Phil. Soc.*, **56**, 406, 1917.

[6] *Pub. A.S.P.*, **27**, 239, 1915.

[7] *Ap. J.*, **63**, 236, 1926; *Mt. W. Contr.*, No. 310.

[8] *Pub. A.S.P.*, **51**, 113, 1939.

[9] We are indebted to Dr. G. E. Kron for helping with this calibration.

52

Aller 1942 spectra of M33 HII regions

Astrophysical Journal, vol. 95, p.52

THE ASTROPHYSICAL JOURNAL, **199**: 591–610, 1975 August 1

SPECTROPHOTOMETRIC OBSERVATIONS OF IONIZED HYDROGEN REGIONS IN NEARBY SPIRAL AND IRREGULAR GALAXIES

HARDING E. SMITH*
Astronomy Department, University of California, Berkeley
Received 1974 November 18; revised 1975 February 6

ABSTRACT

A program of direct photography and spectrophotometry has been carried out on H II regions in a selection of nearby spiral and irregular galaxies. Abundance analyses for H II regions in M101 and M33 show a strong radial gradient in the O/H ratio, decreasing by approximately a factor of 10 across the galaxy disks. The Ne/O and S/O abundance ratios are constant. The derived nitrogen abundances, coupled with the line ratios for other H II regions, indicate a weak gradient in the ratio of N/O, decreasing by about a factor of 4 from the nuclear regions outward. No large helium abundance differences are observed, although the most oxygen-poor regions may show marginally significant helium deficiencies. Excitation differences among the H II regions of Sbc–Scd–Irr galaxies can best be understood in terms of an abundance sequence which progresses from higher to lower heavy-element enrichment as one progresses from the earlier to later type galaxies.

Subject headings: abundances, nebular — galaxies — nebulae

I. INTRODUCTION

The ionized hydrogen regions that define the arms of late type spiral galaxies have an emission-line spectrum that is a one parameter sequence, characterized by the "excitation," defined as the logarithmic ratio of [O III] λλ4959, 5007 to Hβ. The excitation is in turn related to the radial distance of the H II region from the galaxy nucleus, in the sense that the forbidden oxygen lines are stronger in regions farther from the galaxy center. This effect was first noted by Aller (1942) for the H II regions in M33. Other line intensity ratios vary with radial distance as well; Burbidge and Burbidge (1962) showed that the ratio of [N II] λλ6548, 6583 to Hα is much larger near the nuclei of spiral galaxies than in the outer galaxy disks. Using a simple H II region model, Searle (1971) has explained these emission-line gradients by a general abundance gradient across the galaxy disks. Searle requires a decrease in the abundance of oxygen relative to hydrogen of about a factor of 2, and in nitrogen relative to oxygen of a factor of 10, from the nuclear regions to the outer disks in M33 and M101 in order to explain the observed differences in the spectra of these regions.

In this paper we present the results of a detailed photographic and spectrophotometric study of H II regions in nearby spiral and irregular galaxies in an attempt to sort out the effects of abundances, effective temperature of ionizing radiation, and dust content as factors determining the spectral properties of these H II regions. We believe that we are dealing with a homogeneous group of objects; they are all large ($d \geqslant 50$ pc), low-density regions ($n_e \leqslant 500\ \mathrm{cm}^{-3}$ from forbidden line ratios of Searle 1971, Comte and Monnet 1974, and this work) which must be ionized by large associations of O and B stars. This is in contrast to the more familiar nearby H II regions such as the Orion Nebula, M42. Orion is much smaller: even including the outer, low surface brightness regions, it would be barely resolved at the distance of M33, and the electron densities for the highest surface brightness regions are greater than $10^4\ \mathrm{cm}^{-3}$.

We have determined abundances of oxygen, nitrogen, neon, sulfur, and helium for nine H II regions in M101, M33, and NGC 6822. These calculated abundances provide a framework within which the emission-line intensities of a larger sample of H II regions may be understood. Our results qualitatively confirm the conclusions of Searle, showing, however, a steeper gradient in O/H and a consequently smaller N/O gradient across these galaxy disks. In the final sections we discuss the implications of our conclusions with respect to our current understanding of the production of the heavy elements and the evolution of galaxies.

II. DIRECT PHOTOGRAPHY

A program of direct interference filter photography was carried out in 1973 March and April, using the Kitt Peak National Observatory No. 1 36-inch (92 cm) telescope with a 90 mm ITT single-stage, magnetically focused image tube at the f/7.5 focus. Each galaxy was photographed through three filters: 50 Å bandpass (FWHM) interference filters centered at Hβ and λ5007 of [O III], as well as a broad-band blue filter (Corning CS-57 + Schott GG 385) covering the wavelength

* Visiting Astronomer, Kitt Peak National Observatory, which is operated by the Association of Universities for Research in Astronomy, Inc., under contract with the National Science Foundation.

591

© American Astronomical Society • Provided by the NASA Astrophysics Data System

e.g. Smith 1975: HII Reg emission-line gradients

HII regions methodology: *state of the art*

* Standard ***(direct) abundance* derivation in HII regions:**
Study of **chem. parameters & massive stars** (**in 3D/2D)**
T_e fluctuations - Chemical (in)homogeneity

* Chemo-Dynamical-Evolutionary **effects on gal. *abundance gradients*** ... *Tests:* ***2D chemical* galaxy maps**.
(e.g. *Fabian Rosales' Thesis*)

* ***Geometry: 3D* HII region**s (Ercolano, B. et al 07)
Test: **2D ionisation structure constrains 3D photo-ion models**
(e.g. NGC 595, *Monica Relaño et al 2009*)

- ***>>> Ionising star/clusters SEDs.***
- Dependence on: metallicity, masses, evolutionary stage, … ?
  Tests: Gradients of ***radiation hardening*** in galaxies ?
  selected sample of galaxies (**optical & MIR**)

Rewriting the ionisation equation:

$$\frac{n(X^{i+1})}{n(X^i)} = \frac{uc\langle\sigma^i\rangle}{\beta(X^i)} \frac{\int_{\nu(X^i)}^{\infty} F(\nu)\, d\nu/h\nu}{\int_{\nu(\mathrm{H\,I})}^{\infty} F(\nu)\, d\nu/h\nu}$$

A radiation softness parameter **η** can be defined:

region spectrum, an optical "radiation softness" parameter was defined as:

$$\eta = \frac{O^+/O^{2+}}{S^+/S^{2+}} \qquad (2)$$

which does not show a strong dependence on the electron temperature and it is proportional to the corresponding ratio based on the emission lines,

$$\eta' = \frac{I([\mathrm{O\,II}]\lambda3727)/I([\mathrm{O\,III}]\lambda\lambda4959,5007)}{I([\mathrm{S\,II}]\lambda\lambda6717,6731)/I([\mathrm{S\,III}]\lambda\lambda9069,9532)} \qquad (3)$$

This can be expressed as a **function of the stellar Teff** or of the equivalent quantity corresponding to the SED of a given cluster, provided a family of model atmospheres is assumed

(after Vilchez & Pagel 1988)

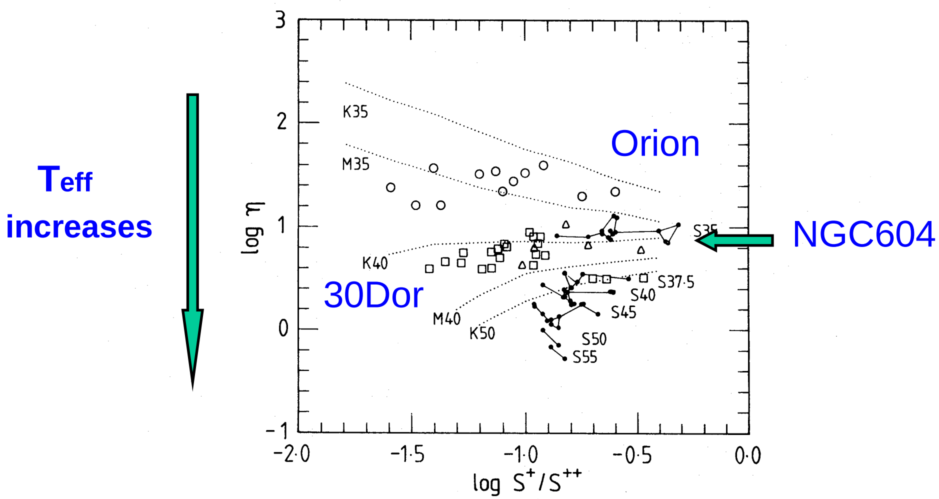

Figure 1. Spatially resolved observations of the Orion Nebula (open circles; Peimbert & Torres-Peimbert 1977), 30 Dor (squares; Rosa & Mathis 1987), and NGC 604 (triangles; Diaz *et al.* 1987), over a plot of log η versus log S^+/S^{++}. Photoionization models by Mathis are represented by dotted lines labelled with the atmospheres used (M: Mihalas; K: Kurucz log $g = 4$) and their effective temperature in units of 10^3 K. Black dots represent individual H II region models after S80. Each set of S80 models with the same T_{eff} is connected by a continuous line and labelled with S (Stasinska) and their value of effective temperature in units of 10^3 K.

U-independent to 1st order; neglecting charge exchange reactions & assuming ionization bounded nebulae. Very low sensitivity to Te and Ne & reddening independent.

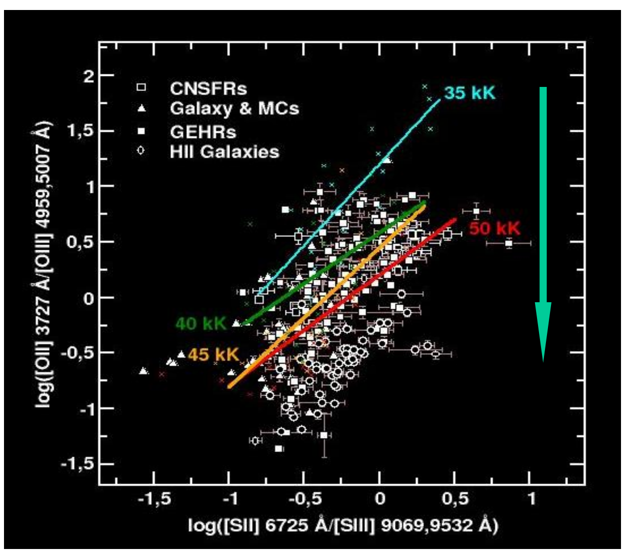

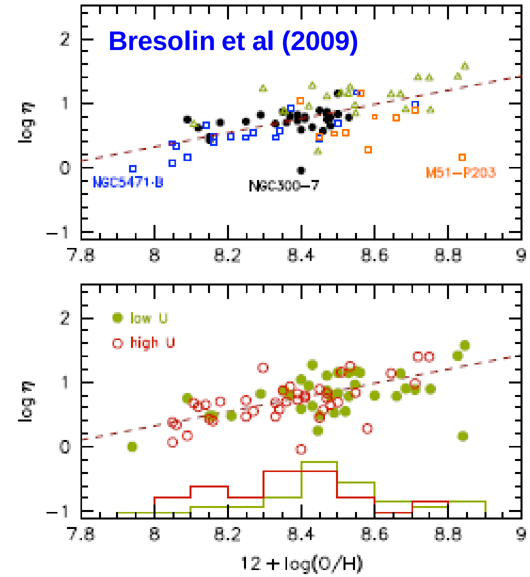

FIG. 14.— *(Top)* The dependence of log η on O/H for the same sample of H II regions shown in Fig. 13. We identify NGC 5471 in M101, NGC 300-7, and M51-P203 as three objects with particularly hard ionizing spectra. The least-square fit to the data points, excluding NGC 300-7 and M51-P203, is shown by the dashed line. *(Bottom)* Same diagram as above, using different symbols to separate H II regions with low and high ionization parameter U, adopting the median S^+/S^{++} ionic ratio as the cut-off value. The histograms at the bottom, drawn at an arbitrary scale, display the distribution of the two

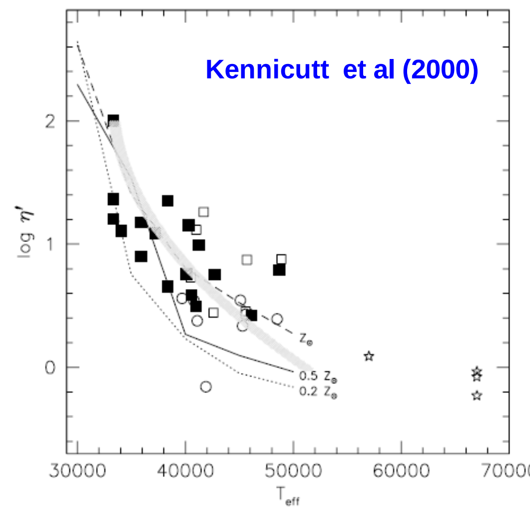

FIG. 13.—Dependence of the ionization hardness parameter η' (eq. [2]) and stellar effective for the H II regions in this sample, with symbols coded as in Fig. 4. The lines show photoionization model sequences for oxygen abundances of 0.2, 0.5, and 1.0 $Z_{\odot}$. The dashed line shows a quadratic empirical fit to the data.

Hardening of the ionising photons in HII Regions across spiral disks:

the slope of the gradient as a new galaxy parameter

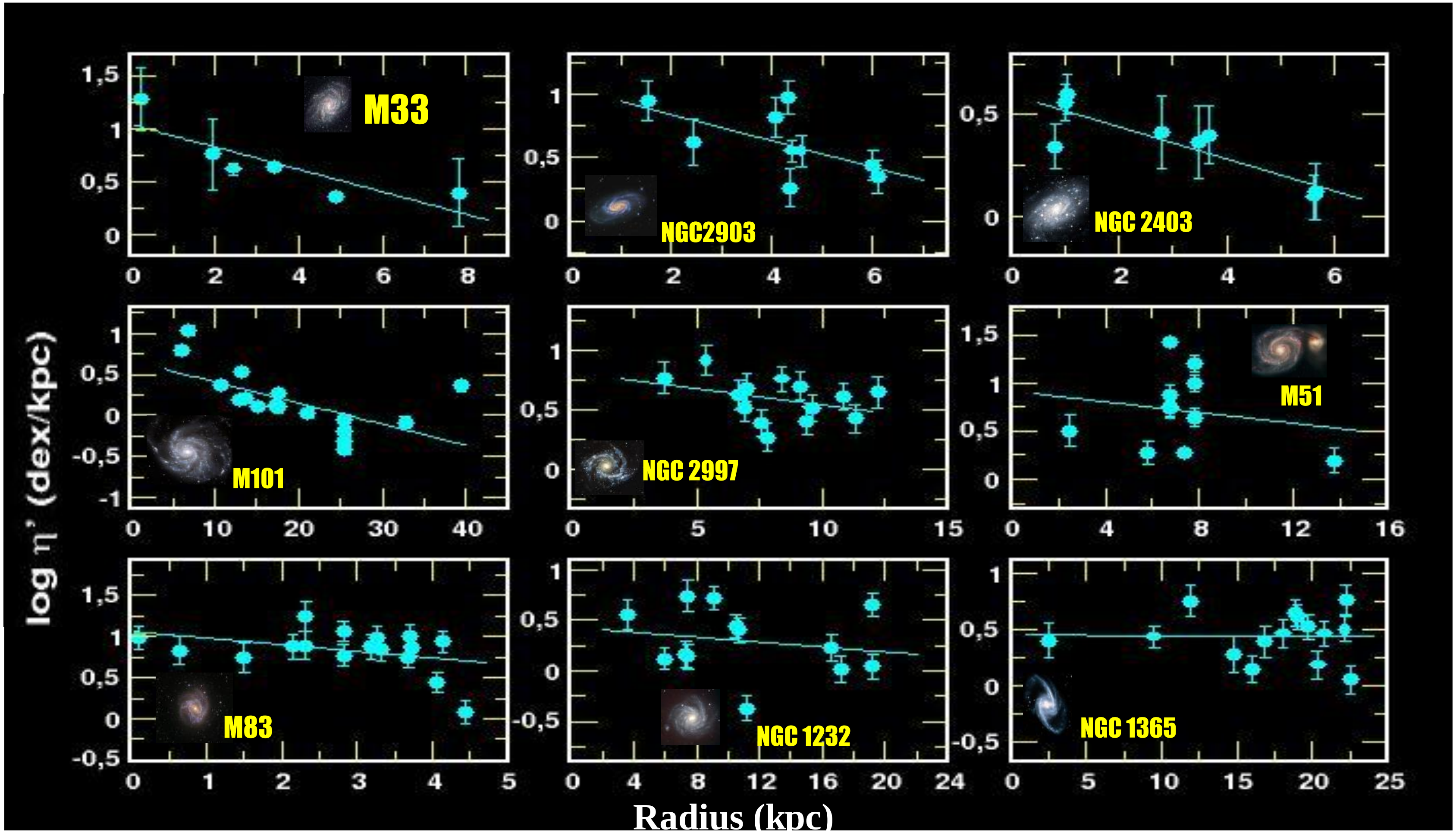

Perez-Montero & Vilchez (2009) *MNRAS*

The radiation softness parameter **η methodology** has been **extended to the MidIR** domain (ISO; Spitzer)

Among others: N. L. Martin-Hernandez (PhD 2002; and latter work with cols.); also K. Morisset (2004a,b)

Convenient ionic ratios used to define η_{MIR} are e.g.

[NeIII/II]15.5/12.8µm

[SIV/III] 10.5/18.7µm,

[ArIII/II]8.98/6.98µm

[NIII/II]57.3/121.8µm

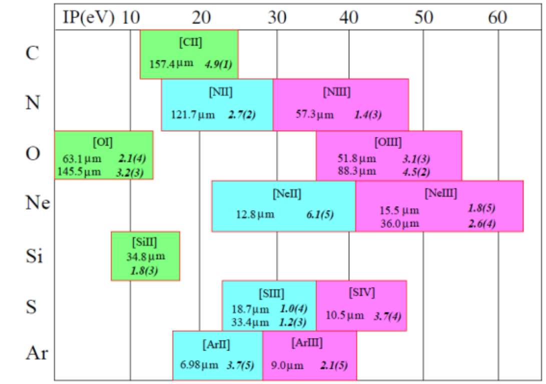

Fig. 1. The fine-structure atomic lines observed in the combined ISO SWS/LWS spectra of compact H II regions are shown as a function of the ionization potential. The electron critical densities, indicated for every line in italic, are given in units of cm^{-3} and are expressed as $a(b) = a \times 10^b$. The critical densities for the ions with ionization potential lower than 13.6 eV (emitted in the photodissociation region) are taken from Tielens & Hollenbach (1985). The other critical densities were calculated using the latest atomic parameters (see Table 1).

Using most recent Spitzer data, have a look to recent work by:
Lei et al (2009) for BCDs; Le Bouteiller et al (2008) for 30Dor, N66 and NGC3603;
Rubin et al (2008) for M33, among others.

At present, direct derivation of **absolute values of Teff** is a function of the model atmospheres used, so therefore **η** will give a model dependent --e.g. WMBasic, CMFGEN, TLUSTY, FASTWIND, CoStar-- output for present state of the art.

However, a **relative scale of Teff/SED's** could be produced so ranking the ionising star clusters e.g. in HII regions across spiral disks

Gradients of the photon hardening in the MIR: *few galaxies; further data are needed*

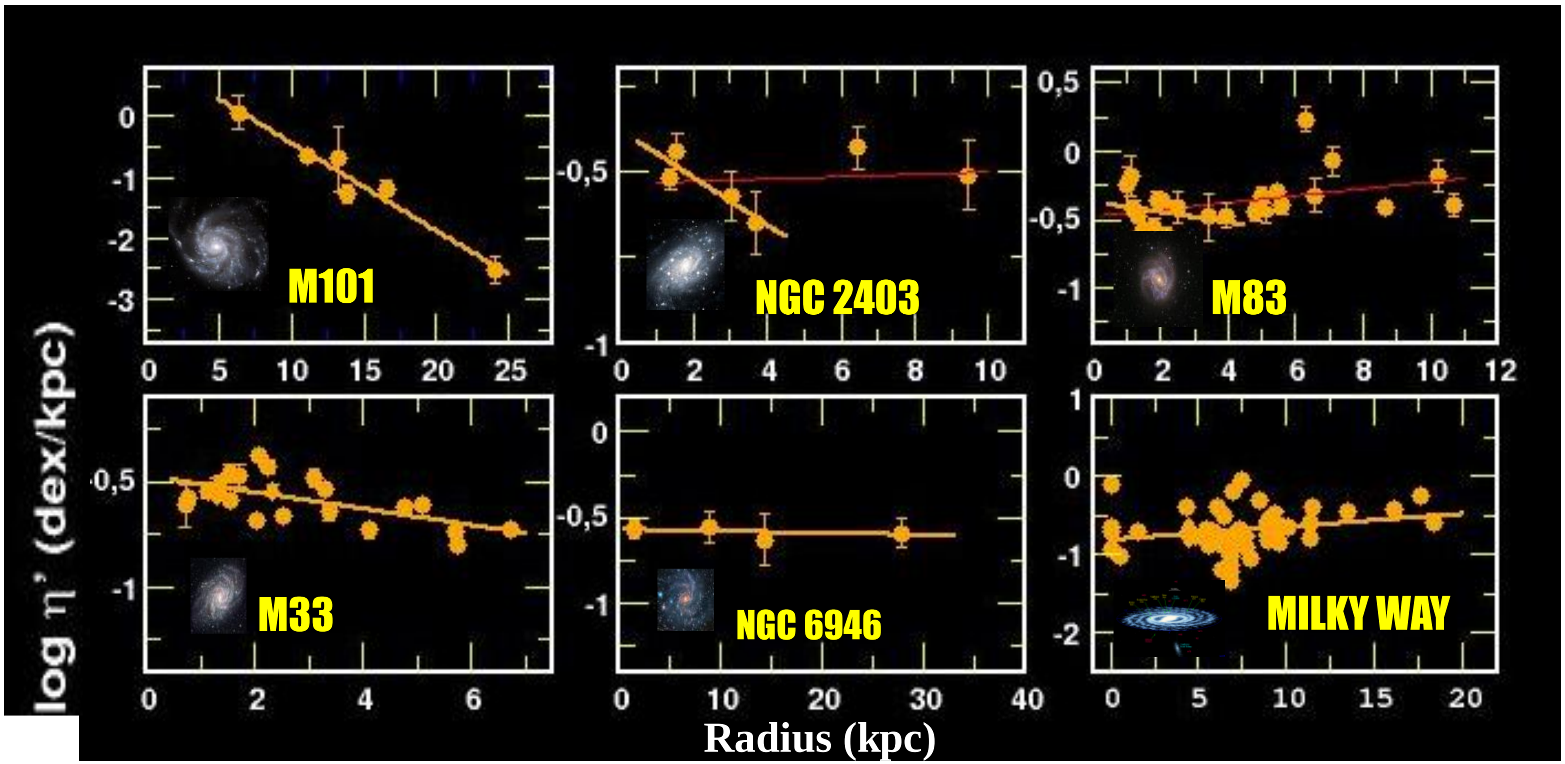

Gradients of ionising photons hardening in massive star clusters vs. galaxy properties: *interpretations*

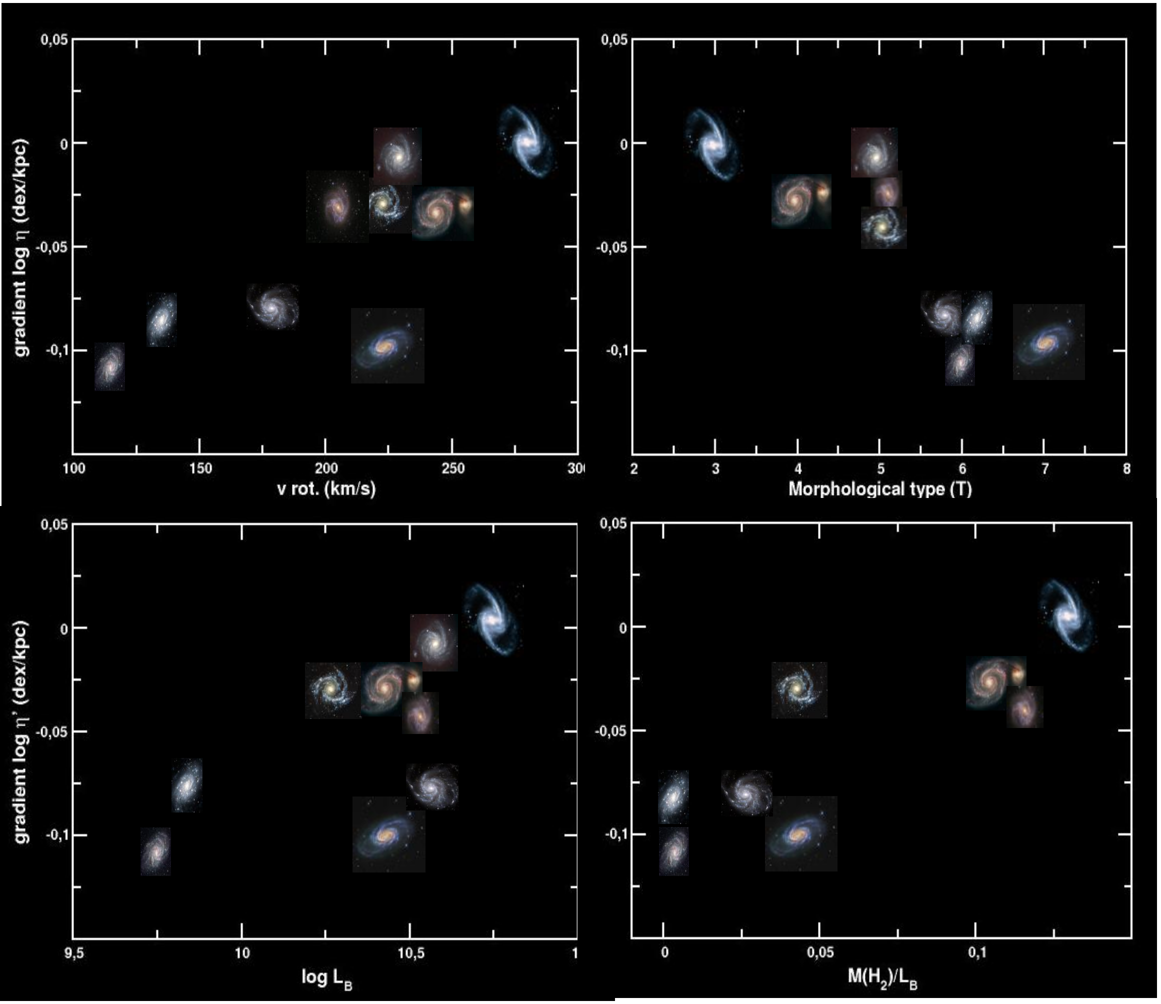

Metallicity is not the main driver of the observed change in the star clusters equivalent effective temperature T_* : O Stars Teff changes by ~ 4000 K from the metallicity of the Magellanic Clouds to typical values for the Milky Way (Massey et al 2009).

It is suggested that star formation is modulated across the spirals disks Observed, so leading to correlations of the gradient of T_* with:

Morphological Type
Galaxy Mass
Mass(H_2) /L_B

An interpretation somewhat speculative could be e.g. linked to recent claims for the max. stellar mass in a cluster being a function of total cluster mass (Weidner, Kroupa & Bonnell 2009)

THANK YOU!

B. Pagel

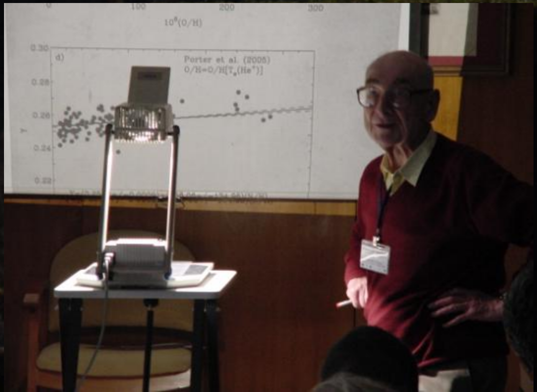

Enrique Perez-Montero
Monica Relaño
Ana Monreal, R. Kennicutt
Carol Kehrig, Angeles Diaz
& *Estallidos*

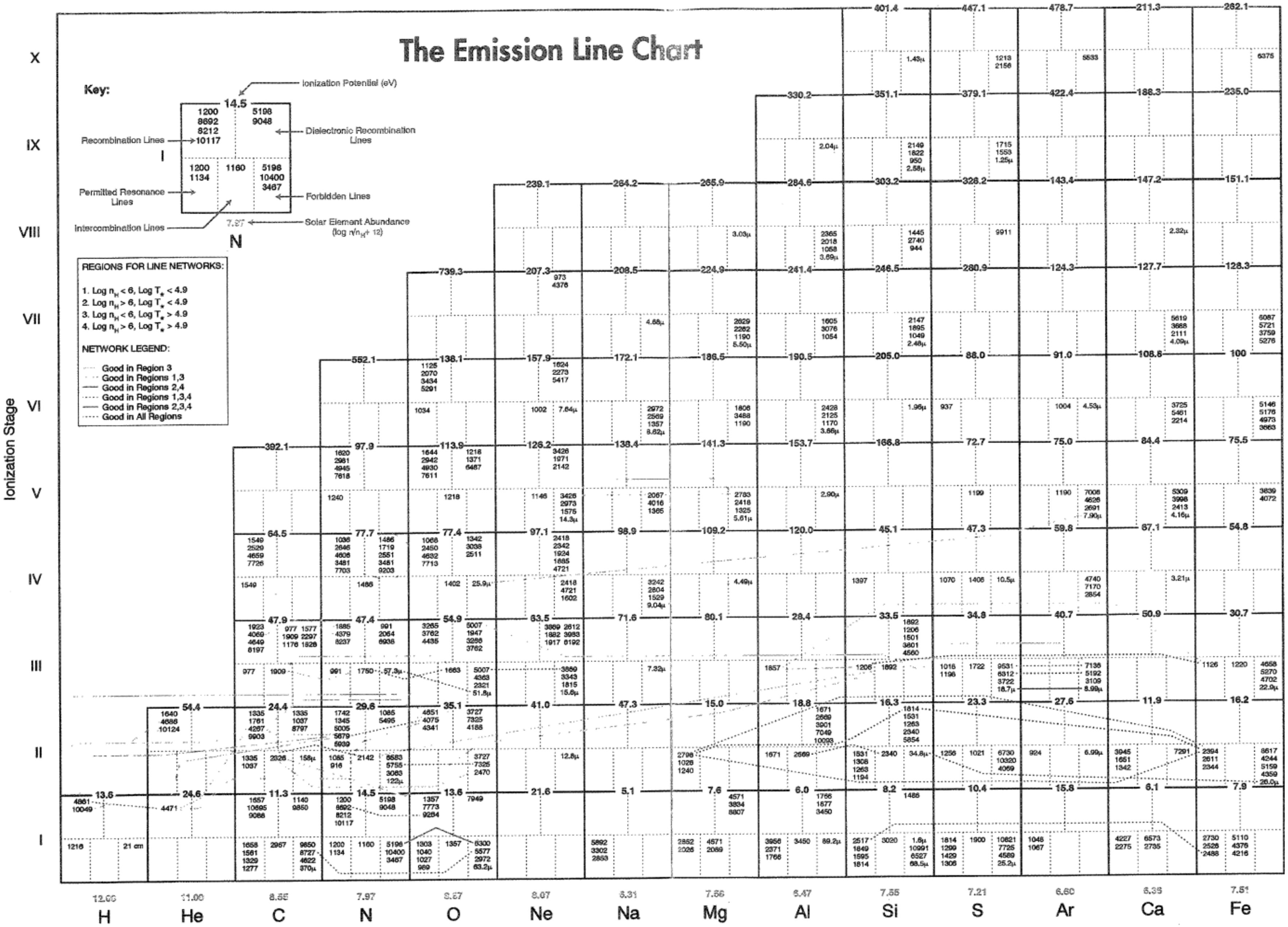

The Emission Line Chart
Key:
Ionization Potential (eV)
Recombination Lines
Dielectronic Recombination Lines
Permitted Resonance Lines
Forbidden Lines
Intercombination Lines
Solar Element Abundance (log n/n_H + 12)
REGIONS FOR LINE NETWORKS:
1. Log n_H < 6, Log T_* < 4.9
2. Log n_H > 6, Log T_* < 4.9
3. Log n_H < 6, Log T_* > 4.9
4. Log n_H > 6, Log T_* > 4.9
NETWORK LEGEND:
Good in Region 3
Good in Regions 1,3
Good in Regions 2,4
Good in Regions 1,3,4
Good in Regions 2,3,4
Good in All Regions
Ionization Stage
X
IX
VIII
VII
VI
V
IV
III
II
I
12.00
H
11.00
He
8.55
C
7.97
N
8.87
O
8.07
Ne
6.31
Na
7.58
Mg
6.47
Al
7.55
Si
7.21
S
6.60
Ar
6.36
Ca
7.51
Fe

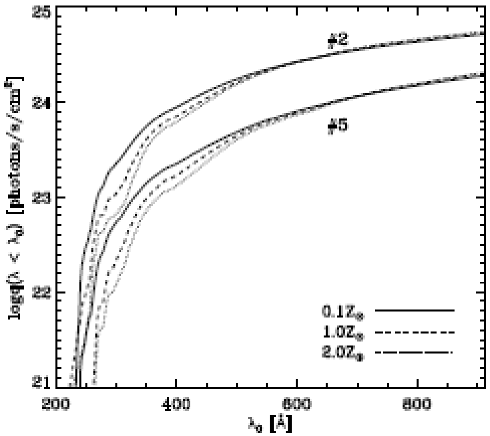

Fig. 4. The effect of the metal content on the number of photons in $\mathrm{cm^{-2}\,s^{-1}}$ below a certain wavelength λ_0 is plotted as a function of this wavelength λ_0. The effect is shown for models #2 and #5.

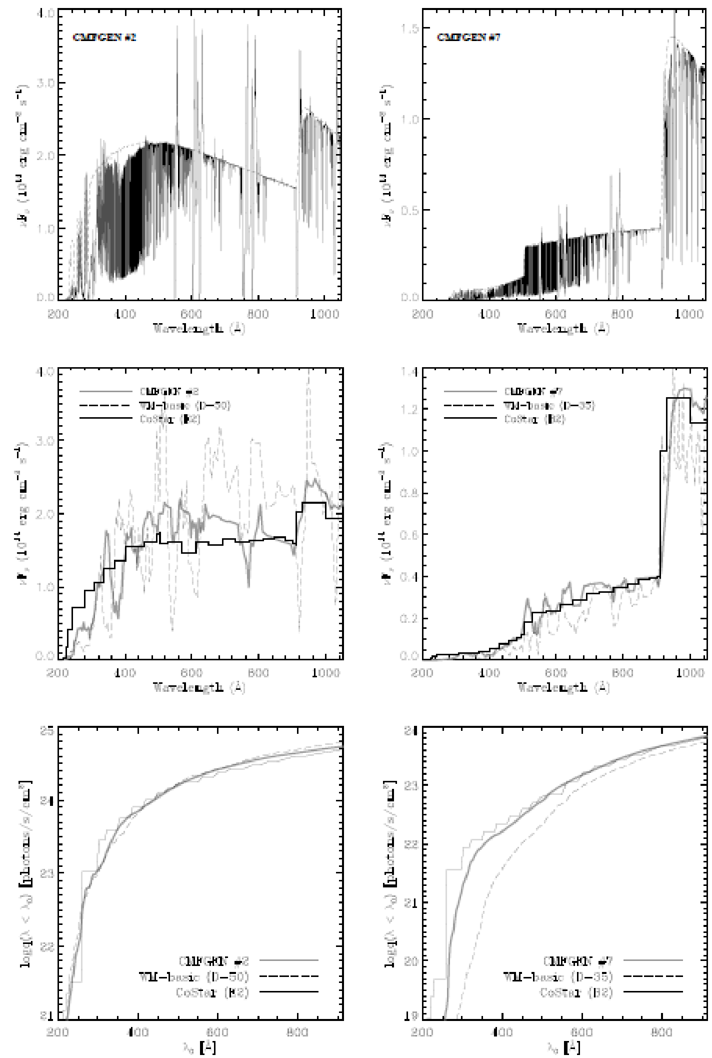

1. (*Top panel*) Emergent SED for models #2 ($T_{\rm eff}$ = 48 670 K) and #7 ($T_{\rm eff}$ = 35 900 K). The continuum is plotted by a ed line. (*Middle panel*) Comparison of the emergent SED for models #2 (left panel) and #7 (right panel) with CoStar and -basic dwarf models at similar $T_{\rm eff}$. (*Bottom panel*) The number of photons in $\mathrm{cm^{-2}\,s^{-1}}$ below wavelength λ_0 calculated from odels considered in the middle panel is plotted as a function of this wavelength λ_0.

Table 5. Predicted number of ionizing photons Q_0 and Q_1 for # 2 and #5 as a function of metal abundance.

	Model #2		Model #5	
$Z/Z_\odot$	$\log Q_0$	$\log Q_1$	$\log Q_0$	$\log Q_1$
2	49.70	49.16	49.09	48.40
1	49.69	49.18	49.08	48.44
1/2	49.69	49.19	49.07	48.46
1/5	49.68	49.20	49.07	48.47
1/10	49.67	49.21	49.06	48.48

M. R. Mokiem[1], N. L. Martín-Hernández[2] ⋆, A. Lenorzer[1], A. de Koter[1], and A. G. G. M. Tielens[2,3]
2004 A&A

HII regions Geometry & Ionisation structure tests to 3D photo-i models

$\exists$ internal T_e gradients; extinction & dust distribution; geometrical distribution of massive ionising clusters …

=> **DETAILED IFU STUDY OF NGC 595 IN M 33**

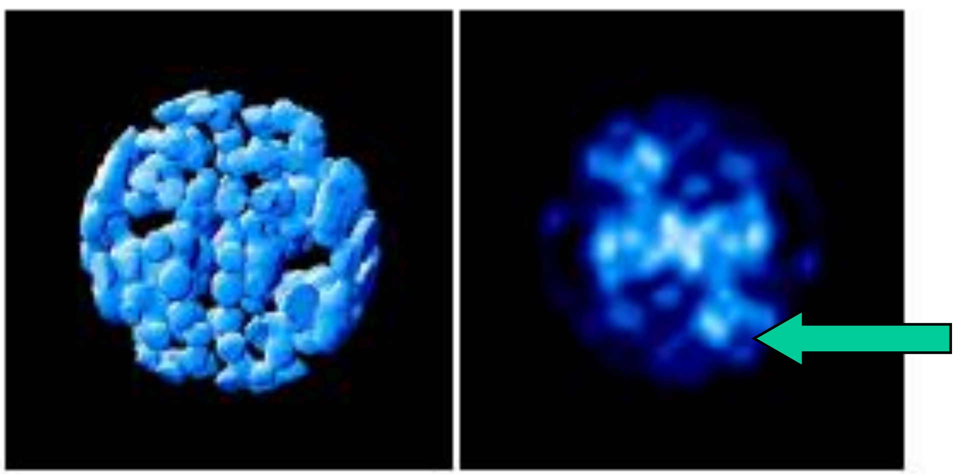

Figure 1. The left panel shows a 3D representation of the Strömgren sphere distribution for case F, plotted as the iso-surfaces where the ionisation fraction of hydrogen is 0.95. The adjacent right panel shows an average projection map of the ionic abundance of H^+.

3D montecarlo photo-ionization models: ionising stars distribution (Ercolano, B. et al. 2007)